Modeling sediment sources and yields in a Pyrenean catchment draining to a large reservoir (Ésera River, Ebro Basin)

Leticia Palazón & Ana Navas

Abstract

Purpose: The study aimed to use the Soil and Water Assessment Tool (SWAT) model to simulate erosion processes in an alpine–prealpine catchment in order to provide data and information that may be relevant for managers so as to minimize reservoir siltation and water quality degradation. The main objective was to assess sediment production across the catchment and sediment supply to the main reservoir.

Materials and methods: The Barasona reservoir catchment (1,509 km^2) is located in the Central Spanish Pyrenees, in the Ebro Basin. This catchment was selected for the case study given the regional significance of the Barasona reservoir and its siltation problems. The catchment has a mountain climate, with strong altitudinal and north–south gradients. The catchment is characterized by heterogeneous topography and lithology, resulting in a varied mosaic of slopes, soil types, and land covers. The Jueu karst system and two small headwater reservoirs were parameterized and calibrated in the model. The SWAT model sediment calibration for the catchment was based on a prior monthly hydrologic calibration, and the model validation was based on the sediment depositional history of the Barasona reservoir.

Results and discussion: The simulation period (2003–2006) and the validation period (1993–2002) produced average sediment yields to the reservoir of 643,000 and 575,000 t year−1, respectively. Large variations in sediment production were found between the subcatchments in the Barasona catchment due to differences in rock outcrops, land cover, and slope gradient. Sediment loss in the Jueu karst system was 15,500 t and the two small headwater reservoirs retained 31,200 and 50,300 t. Sediment production in relation to precipitation showed high temporal variability, with specific sediment yields to the Barasona reservoir ranging from 2.74 to 8.25 t ha−1 year−1. Strong lithological control was observed for sediment production in the subcatchments. The main sediment sources were located in the badlands developed on marls in the middle part of the catchment (internal depressions).

Conclusions: The proposed model has proved useful for identifying areas where significant erosion processes take place in large alpine–prealpine catchments at a regional level and also for assessing discharge losses by the karst system and the sedimentary role of the small reservoirs. The information obtained through this research will be of interest in assessing the spatial distribution of sediment

sources and areas of high sediment yield, which will be useful to establish criteria for remediation strategies.

Keywords: Sediment yield; Reservoir siltation; SWAT model; Alpine–prealpine; Large catchment; Ésera and Isábena Rivers; Mediterranean region.

1 Introduction

Within a river system, a dam can significantly affect the balance of sediment inflow and outflow in the impounded reach, resulting in low flow velocities and efficient sediment trapping (Mamede et al. 2006). Although sediment has a variety of diverse roles and its regulation and management are complex, it is accepted that reservoir siltation is one of the worst off-site consequences of soil erosion and sediment delivery (Navas et al. 2004) and its effects can be economically serious. Reservoir siltation reduces the water storage capacity and life span of reservoirs, and it affects electricity production and flood control capacities, increasing maintenance costs (Garbrecht and Garbrecht 2004). In addition, as a by-product of human activities upstream of the dam, the fine fraction of the incoming suspended sediments may carry adsorbed pollutants and their deposition may have environmental consequences (Mamede et al. 2006). Hence, information on water-induced soil erosion and sediment export is essential in order to implement management practices that are better designed to prevent reservoir siltation (Molino et al. 2007).

In the Central Spanish Pyrenees, there is a great diversity of geomorphic processes related to soil erosion and sediment yield due to topographic and climatic heterogeneity and altitudinal gradient. Human activity during the last 4,000 years has contributed to the disturbance of the original landscape and its hydromorphological dynamics (Navas et al. 1997; García-Ruiz and Valero-Garcés 1998). In the last century, many Spanish Pyrenean rivers have been dammed to provide electricity and irrigation water for Mediterranean lowland areas. The rugged topography, frequent floods, and changes in land use over the last few decades have triggered soil erosion and consequently the siltation of reservoirs and created off-site environmental problems (Valero-Garcés et al. 1999; Navas et al. 2009). Changes in both hydrological regimes and the supply of sediment loads have been recorded in Pyrenean dammed rivers and lakes (Morellón et al. 2011; Navas et al. 2011). Sediment delivery from headwater catchments to reservoirs poses a serious threat to reservoir sustainability and is a critical issue in Mediterranean environments where water resources are scarce (López-Vicente et al. 2011). Specific sediment yield in the northern part of the Ebro Basin, Spain (Pyrenean region, 370 t km^{-2} $year^{-1}$) is five times higher than that in the southern part of the Ebro Basin (Iberian Massif, 78 t km−2 year−1), reflecting the particular hydromorphic conditions of the Pyrenean region (Batalla and Vericat 2011).

Environmental concerns about these fragile systems have stressed the need to gather information on water-induced erosion processes linked to hydrological systems in mountain environments.

Continuous direct measurements with sufficient spatial coverage are difficult to obtain in mountain ecosystems; therefore, a robust computational model, such as the Soil and Water Assessment Tool (SWAT), that simulates hydrological and sedimentological processes, can offer an effective means to study land surface dynamics (Stratton et al. 2009). Modeling runoff and sediment transport at the catchment scale is a key instrument for predicting sediment yield with the aim of preserving soil and water resources. Although most erosion and sediment deposition processes have already been studied in detail, modeling the association between on-site soil erosion and total sediment yield at the outlet of a catchment often problematic, not only due to the difficulties involved in modeling a cascading system but also because of the lack of detailed data at the regional scale with which to parameterize and calibrate/validate models as continuous sediment yield measurements. The SWAT model has been extensively applied throughout the world to deal with a wide range of scales and issues related to hydrology, water management, climate change impacts, land use impacts, best management practices, conservation agriculture, sedimentation, and pollution (Gassman et al. 2007). The SWAT has been widely implemented to perform hydrological simulations to estimate streamflow timing and volumes from mountainous catchments worldwide (e.g., Gikas et al. 2006; Zhang et al. 2008; Yu et al. 2011; Rahman et al. 2013). However, there have been few studies that evaluate sediment production in alpine mountain catchments, and despite the work that has been undertaken (e.g., Abbaspour et al. 2007; Rostamian et al. 2008; Flynn and Van Liew 2011), very few studies have been conducted to evaluate sediment production in large alpine–prealpine catchments.

In the present study, we evaluated simulation of sediment movement (i.e., sediment yield) by the SWAT model for the Barasona catchment for the period 2003–2006. A mountain catchment such as the drainage area of the Barasona reservoir (southern Pyrenees) presents a considerable challenge for spatially distributed modeling, due to its highly variable precipitation, an impounded river, a karst system that subtracts discharge, and its significant snowfall–snowmelt processes. Its extreme altitudinal gradients and inaccessibility also contribute to poor data resolution for the parameterization and calibration of the SWAT model. This work was based on findings from a previous hydrological calibration of the model for the catchment with good to very good monthly streamflow simulations. This fact encouraged us to examine the performance of the sediment model in obtaining the sediment yields from the different subcatchments and sediment delivery to the Barasona reservoir. Given the intense erosive processes that have been described in nearby areas of the Pyrenean region, modeling a large catchment such as the Barasona catchment, for which information from bathymetric studies and radiometric data on sedimentation rates are available, would be a sound basis to apply and verify the SWAT model in large mountain catchments.

2 Material and methods

2.1 Study area

The Barasona reservoir catchment (1,509 km^2) is located in the central part of the Spanish Pyrenees, in the basin of the upper Cinca River, a northern tributary of the Ebro River (Fig. 1). The Barasona reservoir (692 ha) was built on the Ésera River in 1932 to supply water for irrigation and electricity generation. Its initial water capacity was 71 hm^3, which was increased in 1972 to a maximum storage capacity of 92 hm^3. The reservoir also supplies water to the Aragón and Cataluña canal, which irrigates more than 100,000 ha. Over the past 65 years, there has been a considerable loss of storage capacity in the reservoir (Navas et al. 1998; Valero-Garcés et al. 1999). A bathymetric survey in 1995 indicated that the reservoir had lost approximately one third of its initial water storage capacity; the volume of accumulated sediment in the reservoir was about 16–18×10^6 m^3, with a maximum thickness of 20–25 m near the dam wall (personal communication).

The catchment altitudes range from 424 m above sea level (a.s.l.) at the catchment outlet (Barasona reservoir) to 3,404 m a.s.l. at the headwaters (Aneto Peak). The mean catchment slope is 39 %, and it has a mean elevation of 1,313 m a.s.l. The area, characterized by its abrupt topography, is formed by five main Pyrenean structural units (WNW–ESE-trending geologic units) arranged from north to south as follows (Fig. 2): the axial Pyrenees, mostly composed of competent rocks, with large mountain bodies and the highest Pyrenean peak (Aneto Peak); the internal ranges composed of large packages of limestones that have developed deep, narrow gorges; the internal depressions, located in a previous structural unit, comprising depressions formed on more erodible materials which develop badlands on marls; the intermediate depression, a relative lowland area composed of detrital sedimentary rocks; and the external ranges that delimit the catchment to the south. The lithological competence of the structural units controls the distribution of the geomorphological processes, slope ranges, and, to some extent, the location of agricultural fields. The distribution of slope range and percentage of competent lithology decreases in the structural units from the axial Pyrenees unit to the external ranges, while the percentage of cultivated fields increases (Fig. 2).

The catchment climate is defined as mountain type, wet and cold, with both Atlantic and Mediterranean influences (García-Ruiz et al. 2001). Temperature and precipitation gradients are observed for both north–south and west–east regions according to the relief and to the climate influences of the Atlantic Ocean and Mediterranean Sea. The topographic heterogeneity of the region partly explains the great spatial variability in annual precipitation (Verdú et al. 2006a), which ranges from 500 mm at the outlet to >2,500 mm on the divides (>3,000 m a.s.l.) (García-Ruiz et al. 2001).

Temperatures are mainly dictated by the altitudinal gradient, and the temperature gradient has been estimated to be around −5 °C km^{-1} (e.g., García-Ruiz et al. 2001). As a result, the mean annual temperature ranges from 12 °C at the Barasona reservoir (424 m a.s.l.) to <4 °C in the areas >2,000 m a.s.l.

The drainage network is formed by two main rivers, the Ésera River and its main tributary, the Isábena River. Part of the Ésera headwaters was removed as effective drainage area because it drains underground, toward the Jueu karst system to the Garonne River (Arán Valley, Spain). The Isábena is a non-regulated river whereas the Ésera River has small reservoirs, canals, and dams for hydropower purposes. The study area has a transitional nival–pluvial hydrologic regime, characterized by two maxima (García-Ruiz et al. 2001): the first during the spring period (April–June) due to snowmelt and the second during late autumn (October–November) due to precipitation. High slopes and the presence of deep, narrow gorges favor rapid runoff and large floods that are caused by different mechanisms: late spring–early summer snowmelt and summer thunderstorms, and heavy rains in late autumn.

In general, the catchment soils are stony and alkaline, overlying fractured bedrock with textures ranging from loam to sandy loam. Soils are mostly shallow (<0.6 m) and generally well-drained with limited average water content and moderate to low structural stability.

2.2 The Soil and Water Assessment Tool (SWAT) model

The SWAT model is a physically based, semi-distributed, agro-hydrological model, which operates on a minimum of a daily time step and at the catchment scale. The SWAT is designed to predict the impact of management on water, sediment, and agricultural chemical yields in ungauged catchments (Arnold et al. 1998). The model is capable of continuous simulation for dissolved and particulate elements in large complex catchments with varying weather, soils, and management conditions over long time periods. Theory and details of the different processes integrated in the SWAT model are available online in SWAT documentation (http://swatmodel.tamu.edu/).

In this study, the SWAT2009 version (release 93.6) of the model was used in conjunction with the geographical information system (GIS) software package ArcMAP (9.3; ESRI). ArcSWAT (Olivera et al. 2006) is a GIS-based graphical user interface that can be downloaded from the SWAT model website (SWAT 2011). It facilitates catchment delineation, subdivision, and parameterization.

2.3 The Barasona catchment model setup

2.3.1 Model input

The SWAT model relies on discretization of unique hydrological response units (HRUs) that are defined by distinct combinations of categorized land covers, soil types, and slopes (Table 1). Compiling the input data needed to run the model required considerable work, as well as documenting and adapting the available information, since there were few or no tabulated data to characterize the catchment.

The 22 land cover categories from the Corine Land Cover 2000 (CLC2000) identified in the catchment were evaluated to assign an equivalent class in the SWAT2009 database. The SWAT categories were edited in order to perform their regional characteristics in the model. Soil types were characterized by a user soil database generated from the information on the soil types (Fig. 1). The data required by the model for the 18 soil types related to soil hydrologic group, soil texture, bulk density, available water capacity, saturated hydraulic conductivity, organic carbon content, soil depth, USLE soil erodibility KUSLE factor, and albedo. The soil parameters were defined based on field samples, mathematical models, and field observations for the Barasona catchment. The KUSLE factor was calculated according to a general equation developed by Williams (1995) as per the SWAT handbook (Neitsch et al. 2010). Soil depths were defined based on field observations and set at 0.6 m for developed soils, 0.2 m for minerals soils, and 0.02 m for bare soil where badlands are developed. The bare rock and badlands of the catchment were defined and included in the soil and land cover SWAT2009 database in order to perform their surface characteristics. Delineation of the Barasona catchment, its network, and definition of a slope classification were based on a digital elevation model (DEM, Fig. 1). Given the large slope variations in the catchment, five categories were derived from the DEM to characterize the variety of the different surfaces (Table 1). Finally, the configuration led to 5,399 HRUs being defined within ArcSWAT, based on overlays of land use, soil, and slope input layers.

The minimum SWAT requirements for climate inputs were daily minimum and maximum temperature and rainfall data, which provide the moisture and energy that drive all other processes simulated in the catchment. Thus, daily rainfall records from four stations were selected from a revised database (1955–2006; Vicente-Serrano et al. 2009), and daily temperature records from five stations were obtained from the State Meteorological Agency (AEMET, Fig. 1). Rainfall time series were debugged via a process that included reconstruction, gap filling, quality control, and homogeneity testing (Vicente-Serrano et al. 2009).

The measured streamflow data available for two gauging stations (Graus and Capella) of the Barasona catchment were used to test the hydrological accuracy of SWAT simulations (Table 2). The Graus and Capella gauging stations capture the discharge of the Ésera River (894.2 km^2) and the Isábena River

(428.3 km^2) catchments, respectively (Fig. 1). The Ebro River Basin Authority (Confederación Hidrográfica del Ebro (CHE)) provided the monthly streamflow data.

2.3.2 Model parameterization

Calibration of the SWAT model was necessary as it comprises a large number of parameters that define various catchment characteristics and processes. Automatic calibration for the natural streamflow of the Isábena River was first attempted in a previous study (Palazón and Navas 2011), followed by manual calibration to improve the accuracy of simulated monthly streamflows at the Graus and Capella gauge stations by successive changes in model parameters. Calibration was performed for the most suitable and representative period. The period 2003–2006 was selected after studying records of annual precipitation and streamflow distributions in the Barasona catchment over a 30-year period, given that this period showed variable hydrological conditions which allow suitable calibration of the SWAT model. Based on the annual precipitation measured by the rain gauges and on the annual runoff and its related flow return periods recorded by the stream gauging stations, the study period years were classed as wet (2003), dry (2004), very dry (2005), and intermediate conditions (2006) (Table 2). Monthly time step simulation was selected as suitable to perform the main periods of high floods that correspond to both the snowmelt and the autumn season when most sediment is exported. Calibration performance was evaluated for each change in parameter values via the Nash–Sutcliffe efficiency (NSE) coefficient (Nash and Sutcliffe 1970) using the monthly discharge data of the Graus and Capella gauge stations (Fig. 1). During the calibration process, changes in parameter values were edited to produce values of NSE closer to 1. In this work, the calibration focused on determining a sediment yield to the Barasona reservoir in accordance with that measured by Avedaño-Salas et al. (1997), while maintaining the hydrological calibration. Finally, 17 parameters were modified manually and fixed so as to obtain monthly streamflow values that were in good agreement with the monthly streamflow measured in the watershed and to obtain sediment yields to the reservoir that were in agreement with the bathymetric data. Calibrated parameters related to groundwater definition, snowfall–snowmelt parameterization, and sediment yield are presented in Table 3. The calibration was validated for a 10-year period (1993–2002). A previous warm-up period of 3 years was carried out to initialize the model and provide appropriate initial conditions for groundwater and soil water storage.

Defining the snowfall–snowmelt processes in the SWAT for this mountainous catchment was an important part of the hydrologic calibration. The snowfall and snowmelt routine within the SWAT is governed by a temperature index method controlled by air temperature, snowpack temperature, melt rate, and a measurement of the areal coverage of snow (Neitsch et al. 2010). Due to the lack of a temperature index method and equivalent available snow data for the study area, the calibration

process focused on increasing the quality of the simulated monthly streamflows. The default SWAT values of the snow routine parameters were subsequently modified so as to obtain the best match with the hydrograph. To account for temperature and precipitation elevation gradients, ten homogeneous elevation bands and their estimated altitudinal gradients were defined in each subcatchment. The temperature altitudinal gradient (temperature lapse rate (TLAPS) in the SWAT) was set at −5 °C km^{-1}, and the precipitation altitudinal gradient (precipitation lapse rate (PLAPS) in the SWAT) was defined in relation to the number of elevation bands above 2,000 m a.s.l. It is widely documented that precipitation gradient decreases from 1,000 mm km−1 to almost half that value above 2,000 m a.s.l. in the study region (Rijckborst 1967). Furthermore, as lapse rates in the SWAT could not be defined by elevation bands and because the surface percentages above this altitude vary in the different subcatchments, the PLAPS for the subcatchments was established at 550 to 1,000 mm km^{-1}. Although this was only an approximation of the highly heterogeneous precipitation for the catchment, at present, there are no better solutions to solve this limitation in the SWAT for the study catchment.

The catchment was divided into 58 subcatchments in order to assess sediment production across the catchment. The subcatchments were defined by the downstream shallow hole of the Jueu karst system, the small headwater reservoirs of the Ésera River, the main tributaries that drain the discharge and the sediment yield to the main rivers (Ésera and Isábena), and other points of interest, such as the gauging stations and the inlet point of the Barasona reservoir.

The Renclusa swallow hole of the Jueu karst system was used to delimit the 30-km^2 headwater subcatchment, which drains into the Garonne River (Fig. 1). This represents an average discharge loss of about 3 m^3 s^{-1} from the Ésera River (López-Moreno et al. 2002). To perform the karst system flow and sediment discharge, the SWAT had to drain all of the simulated runoff of the headwater subcatchment outside the catchment (Palazón and Navas 2013).

The small Paso Nuevo and Linsoles reservoirs (Fig. 1), both with a storage capacity of 3 hm^3, regulate 118 and 283 km^2 of the Ésera headwaters, respectively, with an impounded runoff index (IR) of 0.016 and 0.022, respectively, that, as indicated by Batalla et al. (2004), do not produce monthly runoff regulation. Parameterization of these reservoirs in the SWAT was based on their technical characteristics (reservoir area, principal and emergency spillway volume) and simulated controlled outflow–target release. The model computes the outflow of the reservoirs as a function of the desired monthly target storage. The target release approach attempts to mimic general release rules used by reservoir operators. Although the method is simplistic and cannot account for all decision criteria, it can realistically simulate major outflow and low flow periods (Neitsch et al. 2010). Sediment trap efficiency was based on their IR index using the equation developed by Heinemann (1981) for small

reservoirs, which produced values of trap efficiency included in Brune's curve (Brune 1953). The equilibrium sediment concentration of 0.058 and 0.065 g l^{-1} for the small Linsoles and Paso Nuevo reservoirs were manually calibrated to produce 45 and 60 % of simulated trap efficiency, respectively.

Channel parameterization was assumed to be non-erosive, based on the rocky characteristics of the riverbed. The computed loads from the subcatchments and reservoirs were routed through the channel network, and only sediment deposition was determined based on the unique sediment transport capacity of the simulated streamflow. During channel sediment routing, the maximum amount of sediment that can be reentrained was calculated by a linear parameter (SPCON, Table 3), which was manually calibrated to produce a sediment yield in the same range as that observed by Avedaño-Salas et al. (1997).

3 Results and discussion

3.1 Barasona sediment inflow

The simulated monthly streamflow of the study period (2003–2006) revealed the characteristics of the nival–pluvial regime (Fig. 3), which shows an increase of the streamflow during the snowmelt period and low flows in summer and winter. Simulation of monthly discharges at the Graus and Capella gauging stations were satisfactory to very good, with a NSE coefficient of 0.83 and 0.67, respectively. The differences between observed and simulated monthly hydrographs show simulated advanced snowmelt peak flows for the two first years and a general overestimation of the related summer streamflows; this might be due to the climatic limitations of the model for the catchment. The validation period (1994–2002) resulted in a monthly NSE of 0.49 and 0.63 for the Graus and Capella gauging stations, respectively. For the study years, the simulated precipitation for the catchment classified 2003 as wet, 2004 and 2005 as dry, and 2006 as medium-wet years (Table 4). In comparison with a runoff coefficient of 0.05 for the Isábena subcatchment (Verdú et al. 2006b), the simulated runoff coefficient was 0.11 for the entire study catchment.

Applying the SWAT model to the Barasona catchment for the four calibration years allowed the total sediment yield to the reservoir and the relative contributions of each of the main river subcatchments (Ésera and Isábena) (Table 5) to be estimated. The simulated sediment yield (SY) contribution to the Barasona reservoir for the period was 2,573,000 t, which represents a specific sediment yield (SSY) of 4.68 t ha^{-1} $year^{-1}$. The sediment trap efficiency of the Barasona reservoir was 90.15 % (Almorox et al. 1994), and thus, the average simulated sediment trapped in the reservoir was 580,000 t $year^{-1}$ and the corresponding SSY was 4.42 t ha^{-1} $year^{-1}$. Likewise, the simulated SSY for the validation period was 3.76

t ha^{-1} year^{-1}. These values compare well with the estimated average of 3.50 t ha^{-1} year^{-1} based on a bathymetric survey (1932–1996) in the Barasona reservoir (Avedaño-Salas et al. 1997). This result would suggest sound sediment calibration performance in spite of an acceptable difference in SSY that could be due to the different hydrological characteristics between the longer period of the bathymetric survey and the 4-year simulation period of this study.

As expected, the SY for the wet year 2003 (Table 5) was the highest and double the SY of the following 3 years. The SSY was significantly higher than the average estimated from the bathymetric survey, and it was in agreement with the greatest simulated precipitation for that year. The simulated average annual runoff and precipitation for 2003 were the highest for the study period and nearly double the values of the following year, 2004 (Table 4). Simulated precipitation for 2004 was very similar to the precipitation of 2005, but the average annual runoff of 2004 was higher than that simulated for 2005, which was the driest year of the period. As a result, the SSYs of 2004 and 2005 were 14 % higher and 22 % lower, respectively, than the average SSY of the bathymetric survey. The year 2006 had medium-wet conditions with an average annual runoff that was slightly lower than that simulated for 2004 and had higher precipitation than the previous years. The SSY for 2006 was only 7 % higher than that of the bathymetric survey. In spite of the intermediate wetness of 2006, the model performed a lower SSY than that simulated for 2004 because the preceding year (2005) was the driest of the period, and consequently this condition limited runoff for 2006. The runoff time series matched the time series of annual precipitation quite well for the entire period with the exception of the last year, which had the same annual runoff as the average for the period in spite of a higher precipitation record. As Alatorre et al. (2010) indicated, this multi-annual behavior of runoff can be explained by the fact that deep aquifer recharge occurs at a much slower rate than other processes in the hydrological cycle.

The SY of the Ésera River was influenced by the Jueu karst system and by the presence of the two small headwater reservoirs (Palazón and Navas 2013). The parameterized Jueu karst system also performed a SY loss of 15,500 t and a spring discharge of 0.08–3.7 m^3 s^{-1} from the Ésera headwater to the Garonne River. Based on the calibrated trap efficiency for the Linsoles and Paso Nuevo reservoirs, they retained 31,200 and 50,300 t of sediments, respectively, for the 2003–2006 period.

The relative SY contribution of the Ésera subcatchment was almost double that of the Isábena subcatchment for the 4 years of the 2003–2006 period, and the SSYs of both river subcatchments were similar, at around 5.30 t ha^{-1} year^{-1} (Table 5). Due to the fact that the two subcatchments have similar geological and land cover characteristics—except for the alpine part, which is exclusive to the Ésera subcatchment—the SY values reflect the differences of relative size and discharge. For different periods, López-Tarazón et al. (2009, 2012) obtained measurements of 4.14 and 5.27 t ha^{-1} year^{-1} for the Isábena River for the 2005–2008 and 2007–2009 periods, respectively. For the Barasona

catchment, Alatorre et al. (2010) reported similar SY contributions and SSY of 3.73 t ha^{-1} $year^{-1}$ for the period from May 2005 to May 2006 using the WATEM/SEDEM model.

Other authors have obtained good to very good sediment calibration results for SWAT model performance in mountain catchments. For example, Gikas et al. (2006) reported acceptable agreement of predicted and observed sediment yields for a mountainous agricultural catchment in Greece. Abbaspour et al. (2007) described very good agreement between simulated and observed sediment yields in a prealpine catchment in Switzerland. Flynn and Van Liew (2011) also found that the SWAT was suitable for simulation of sediment dynamics in mountainous terrains in the USA.

3.2 Sediment yield from the main subcatchments

The Barasona catchment was divided into 58 main subcatchments in order to assess sediment production from erosion processes across the catchment (Fig. 4). The subcatchments have different characteristics of land cover, soil types, and slope gradients, which result in different sediment productions for each subcatchment (Fig. 4). The SSYs of the subcatchments were classified in the following ranges: <1, 1–2, 2–10, 10–20, 20–50, and >50 t ha−1 year−1; these ranges were denoted as very low, low, medium, high, very high, and extreme, respectively. For the whole simulation period, 25 subcatchments, which represent 36 % of the catchment surface area, produced very low SSY (<1 t ha−1 year−1). Fifteen subcatchments, which account for around 27 % of the whole catchment, produced >2 t ha^{-1} $year^{-1}$. Very high values of SSY (>20 t ha^{-1} $year^{-1}$) were produced by only five subcatchments, which represent 8 % of the catchment area. The subcatchments with the highest sediment production were located in the middle part of the Barasona catchment. Badland erosion rates in this area amount to as much as 302 t ha^{-1} $year^{-1}$ (Martínez-Casasnovas and Poch 1998). The simulated SSYs for the subcatchments of the Isábena River were in the same order of magnitude as the equivalent subcatchments studied by López-Tarazón et al. (2012), although measurements were for a different period that was drier than our simulation with the SWAT.

The distribution of the SSY classes changed during the simulation period in relation to available water. As a result of this, subcatchment sediment production increased to severe values for the wettest year (2003), decreased for the driest year (2005), and showed only a slight increase for the last year (2006) which had medium precipitation conditions (Fig. 4). For the driest year (2005), >65 % of subcatchment SSY was <1 t ha^{-1} $year^{-1}$. However, around 60 % of subcatchment SSY was >2 t ha^{-1} $year^{-1}$ for the wettest year (2003).

3.3 Relating sediment production to the characteristics of Pyrenean structural units

The axial Pyrenees and the external ranges produced the lowest SSY values (9.5 and 8.1 t ha^{-1} $year^{-1}$, respectively), the intermediate depression and the internal ranges produced intermediate SSY values (24.5 and 17.4 t ha^{-1} $year^{-1}$, respectively), and the internal depressions produced the highest SSY value (232.6 t ha^{-1} $year^{-1}$) (Fig. 2). The temporal variability of SSY for most of the units was concordant with the amount of precipitation (Table 6). The axial Pyrenees, with the highest slope gradients, did not produce the lowest SSY for the driest year (2005) because of the relatively high precipitation during that year. With the exception of the external ranges, the SSY for 2003 was approximately double the average SSY for the period.

With regard to sediment transport by the Ésera and Isábena Rivers, the simulated suspended sediment concentration (SSC; grams per liter) shows distinct downstream patterns toward the Barasona reservoir in relation to the Pyrenean structural units. The SSC in both rivers increased downstream mainly due to the type of materials drained, the slope gradient, and the land cover in the Pyrenean structural units (Table 7). Despite the expected downstream dilution effect, the increase in sediment production from the lowland lithologies (with higher erodibility than those of the headwater materials) counteracted the dilution effect. Comparable SSC increases along the Isábena River were reported by Francke et al. (2008). The downstream SSC was significantly lower in the Isábena River at the axial Pyrenees and the internal ranges, but this pattern changed at the internal and intermediate depressions, where the SSC in the Isábena River was much higher than that of the Ésera River. This relatively higher increase in the SSC in the Isábena River appears to be related to the higher discharge in the Ésera River. Furthermore, the Isábena River collected sediment from a subcatchment that had the highest SSY of the Barasona catchment. At the intermediate depressions, the SSCs in both rivers were similar.

The locations evaluated at the end of the axial Pyrenees and the internal depressions for the Isábena River using the SWAT model are equivalent to the Cabecera and Villacarli sections monitored by Francke et al. (2008) and Lopez-Tarazón et al. (2012) and are in the same range of magnitude. However, the SSC measurements for these monitoring sections were instantaneous and for a different period, and therefore, they cannot be directly compared to the simulated average monthly SSC performed by the SWAT.

The SSY statistics for the subcatchments included in each of the Pyrenean structural units showed great spatial and temporal variability (Table 8). Apart from the wettest year (2003), the axial Pyrenees (mainly comprising competent rocks) produced the lowest SSY values (<1 t ha^{-1} $year^{-1}$) for most of the years (2004–2006) (Fig. 4). Despite the competent lithologies (mostly limestones) that form the internal ranges, average SSY displayed a medium value which was more than three times the average

SSY produced by the axial Pyrenees for the period. For most of the period (2004–2006), SSY was generally very low, except for the wettest year (2003) where SSY increased to low medium values. Excluding the internal depressions, the internal ranges had the greatest variability for the period. The internal depressions, mostly composed of Eocene marls in which badlands have developed, had the highest SSY values. Most of the subcatchments within this unit produced SSY >10 t ha^{-1} $year^{-1}$ for the period and had a maximum value of 151.4 t ha^{-1} $year^{-1}$ for the wettest year (2003). The intermediate depression, a relative lowland area with more gentle slopes, produced very low to medium values of SSY, although SSY production varied largely due to the abundance of cultivated land and the nature of lithologies which were of intermediate competence (Fig. 2). The external ranges, composed mainly of tertiary materials (sandstones and conglomerates), produced very low to low SSY values that were in the same range as those for the axial Pyrenees but with a lower variability for the period. In spite of the abundance of less competent lithologies in the external ranges when compared to the axial Pyrenees, the SYs were similar since the precipitation and slope gradients were lower in the external ranges than in the axial Pyrenees.

The evaluation of the simulation of sediment dynamics by the SWAT model was subject to simplified assumptions, a lack of detailed data, and/or constraints in the model parameterization that produced associated errors that must be taken into account. Errors associated with model parameterization and results are related to the scale of the work, the number and distribution of rainfall and gauging stations, the parameterization of the small reservoirs and the karst system, and the scarcity of input data and measured data required to calibrate the model. The spatial distribution of sediment yield and sediment delivery to the reservoir was in good agreement with bathymetric records and other data from previous catchment studies, in spite of the fact that the monthly time step in the SWAT does not display daily peak flows (Rostamian et al. 2008). Although a reliable and revised rainfall database was used in this study, the limited number of rainfall gauging stations for this large catchment, with a highly variable climate, could be considered to represent poorly this mountain environment (Straton et al. 2009). It is possible that this poor distribution of rainfall gauging stations might not represent a realistic spatial distribution of precipitation, and local storm events could either be neglected or performed (Verdú et al. 2006a) thus modifying the SY of the catchment. To overcome this limitation, Fontaine et al. (2002) were the first to introduce elevation bands in the SWAT that permitted the reproduction of estimated climatic altitudinal gradients, contributing to the improvement of hydrologic simulations (e.g., Zhang et al. 2008). In addition to the elevation bands, the compilation of other climatic stations or the use of other climatic data sources (i.e., radar data) could help to reproduce better the spatial variability in climate in mountainous catchments, as reported by Yu et al. (2011). Furthermore, hydrological calibration of the model using more than two river gauging stations could help achieve better model calibration for specific parts of the catchment (Abbaspour et al. 2007), such as the alpine

Ésera headwaters. While limitations in the definition of the Pyrenean structural units were due to the extension of the defined subcatchments, which were also dependent on the drainage limits, results supported the representativeness of the delimited units for this scale of work. Parameterization of the small headwater reservoirs could produce inconsistencies in the related streamflow and sediment trap efficiency since they cannot be controlled by the simplistic method used and, in addition, respond to water availability and demand. Outflow records for the small reservoirs could define better its managed streamflows (Rahman et al. 2013). Limitations in the simulated sediment storage in the river network and its remobilization for this calibration could produce errors in the estimated SYs to the reservoir. Therefore, a detailed parameterization that includes the erodibility and roughness of the river network in the SWAT, especially of the lower part of the Isábena subcatchment that has sediment deposits, would improve the characterization of sediment storage and its movement in the river network.

4 Conclusions

This study assessed the performance of the SWAT model applied to the alpine–prealpine catchment of the Barasona reservoir, where siltation problems have been identified. This catchment is characterized by scarce input data and a highly variable climate which entails significant challenges in SWAT simulation. In spite of this, results showed that satisfactory monthly streamflow calibration and validation were achieved, especially with the parameterization of the elevation bands which reproduced the estimated altitudinal climatic gradients. Detailed studies in this mountainous environment need extensive compilation of climatic data in order to define better its spatial variability.

The sediment calibration (2003–2006) and validation (1994–2002) periods of the model were validated by bathymetric data of the Barasona reservoir. The SWAT model provided reasonable predictions of sediment yield and identified the different sediment source areas, which were in agreement with observations by other authors. Results showed significant spatial and temporal variability in relation to the precipitation and physiographic characteristics of the catchment. Relationships between the SSY (t ha^{-1} $year^{-1}$) of the defined subcatchments were associated with the relative competence of the lithologies within the Pyrenean structural units. This assessment confirmed that the highest sediment production comes from the middle part of the catchment (internal depressions), where badlands on Eocene marls have developed, with a SSY for the study period 30 times that of the lowest sediment production area (external ranges).

The SWAT model has proved to be useful as an initial approach to sediment yield assessment at a regional level and also for selecting priority areas where further analyses should be undertaken. The

information obtained from this research will be of interest to assess the spatial distribution of erosion in large alpine and prealpine catchments. The success of the SWAT model in determining the sediment flux component in this mountainous catchment (with a scarcity of input data, great climatic gradients and an impounded river), as illustrated in this research, affords an opportunity to extend the use of the SWAT model to other catchments in the Pyrenean region.

Acknowledgments

This research was financially supported by the project EROMED (CGL2011-25486).

References

Abbaspour KC, Yang J, Maximov I, Siber R, Bogner K, Mieleitner J, Zobrist J, Srinivasan R (2007) Modelling hydrology and water quality in the pre-alpine/alpine Thur watershed using SWAT. J Hydrol 333:413–430

Alatorre LC, Beguería S, García-Ruiz JM (2010) Regional scale modeling of hillslope sediment delivery: a case study in the Barasona Reservoir watershed (Spain) using WATEM/SEDEM. J Hydrol 391: 109–123

Almorox J, De Antonio R, Saa A, Cruz Díaz M, Gasco JM (1994) Métodos de estimación de la erosión hídrica. Agrícola Española, Madrid, Spain

Arnold JG, Srinivasan R, Muttiah RS, Williams JR (1998) Large area hydrologic modelling and assessment part I: model development. J Am Water Resour Assoc 34:73–89

Avendaño-Salas C, Sanz-Montero E, Cobo-Rayán R, Gómez-Montaña JL (1997) Sediment yield at Spanish reservoirs and its relationship with the drainage basin area. In: Proceedings of the 19th Symposium of Large Dams. ICOLD (International Committee on Large Dams), Florence, Italy, pp 863–874

Batalla RJ, Gómez CM, Kondolf GM (2004) Reservoir-induced hydrological changes in the Ebro River basin (NE Spain). J Hydrol 290: 117–136

Batalla RJ, Vericat D (2011) An appraisal of the contemporary sediment yield in the Ebro Basin. J Soils Sediments 11:1070–1081

Brune GM (1953) Trap efficiency of reservoirs. Trans Am Geophys Union 34:407–418

Corine Land Cover (2000) Available at http://www.eea.europa.eu/data-and-maps/data/corine-land-cover-clc2000-100-m-version-12-2009

Flynn KF, Van Liew MW (2011) Evaluation of SWAT for sediment prediction in a mountainous snowmelt-dominated catchment. Trans ASABE 54:113–122

Fontaine TA, Cruickshank TS, Arnold JG, Hotchkiss RH (2002) Development of a snowfall-snowmelt routine for mountainous terrain for the Soil Water Assessment Tool (SWAT). J Hydrol 262: 209–223

Francke T, López-Tarazón JA, Vericat D, Bronstert A, Batalla RJ (2008) Flood-based analysis of high-magnitude sediment transport using a non-parametric method. Earth Surf Process Landf 33:2064–2077

Garbrecht JD, Garbrecht GKH (2004) Siltation behind dams in antiquity. In: Rogers JR, Brown GO, Garbrecht JD (eds) Water resources and environmental history. ASCE, Reston, USA, pp 35–43

García-Ruiz JM, Valero-Garcés BL (1998) Historical geomorphic processes and human activities in the Central Spanish Pyrenees. Mt Res Dev 18:309–320

García-Ruiz JM, Beguería S, López-Moreno JI, Lorente A, Seeger M (2001) Los recursos hídricos superficiales del Pirineo aragonés y su evolución reciente. Geoforma Ediciones, Logroño, Spain

Gassman PW, Reyes MR, Green CH, Arnold JG (2007) The Soil and Water Assessment Tool: historical development and future research directions. Trans ASABE 50:1211–1250

Gikas GD, Yiannakopoulou T, Tsihrintzis VA (2006) Modeling of non-point source pollution in a Mediterranean drainage basin. Environ Model Assess 11:219–233

Heinemann HG (1981) A new sediment trap efficiency curve for small reservoirs. Water Resour Bull 17:825–830

López-Moreno JI, Beguería S, García-Ruiz JM (2002) El régimen del río Ésera, Pirineo Aragonés, y su tendencia reciente. Bol Glaciol Aragon 3:131–162

López-Tarazón JA, Batalla RJ, Vericat D, Francke T (2009) Suspended sediment transport in a highly erodible catchment: the river Isábena (Central Pyrenees). Geomorphology 109:210–221

López-Tarazón JA, Batalla RJ, Vericat D, Francke T (2012) The sediment budget of a highly dynamic mesoscale catchment: the River Isábena. Geomorphology 138:15–28

López-Vicente M, Lana-Renault N, García-Ruiz JM, Navas A (2011) Assessing the potential effect of different land cover management practices on sediment yield from an abandoned farmland catchment in the Spanish Pyrenees. J Soils Sediments 11:1440–1455

Mamede GL, Bronstert A, Francke T, Müller EN, De Araujo JC, Batalla RJ, Güntner A (2006) 1D process-based modelling of reservoir sedimentation: a case study for the Barasona Reservoir in Spain. In: Rui MLF, Alves ECTL, Leal JGAB, Cardoso AH (eds) Proceedings of the International Conference on Fluvial Hydraulics - River Flow 2006, Taylor and Francis, London, UK, Vol. 2, pp 1585-1594

Martínez-Casasnovas JA, Poch RM (1998) Estado de conservación de los suelos de la cuenca del embalse Joaquín Costa. Limnetica 14:83–91

Molino B, Viparelli R, De Vincenzo A (2007) Effects of river network works and soil conservation measures on reservoir siltation. Int J Sediment Res 22:273–281

Morellón M, Valero-Garcés BL, González-Sampériz P, Vegas-Vilarrúbia T, Rubio E, Rieradevall M, Delgado-Huertas A, Mata P, Romero O, Engstrom DR, López-Vicente M, Navas A, Soto J (2011) Climate changes and human activities recorded in the sediments of Lake Estanya (NE Spain) during the Medieval Warm Period and Little Ice Age. J Paleolimnol 46:423–452

Nash JE, Sutcliffe JV (1970) River flow forecasting through conceptual models part I—a discussion of principles. J Hydrol 10:282–290

Navas A, García-Ruiz JM, Machín J, Lasanta T, Walling D, Quine T, Valero B (1997) Soil erosion on dry farming land in two changing environments of the central Ebro Valley, Spain. In: Walling DE, Probst JL (eds) Human impact on erosion and sedimentation. IAHS Publ 245, IAHS Press, Wallingford, UK, pp 13–20

Navas A, Valero B, Machín J, Walling D (1998) Los sedimentos del embalse de Joaquín Costa y la historia de su depósito. Limnetica 14: 93–112

Navas A, Valero-Garcés BL, Machín J (2004) An approach to integrated assessment of reservoir siltation: the Joaquín Costa reservoir as a case study. Hydrol Earth Syst Sci 8:1193–1199

Navas A, Valero-Garcés BL, Gaspar L, Machín J (2009) Reconstructing the history of sediment accumulation in the Yesa reservoir: an approach for management of mountain reservoirs. Lake Reserv Manage 25:15–27

Navas A, Valero-Garcés BL, Gaspar L, Palazón L, Machín J (2011) Radionuclides and stable elements in the sediments of the Yesa reservoir (Central Spanish Pyrenees). J Soils Sediments 11:1082–1098

Neitsch SL, Arnold JG, Kiniry JR, Srinivasan R, Williams JR (2010) Soil and Water Assessment Tool input/output file documentation: Version 2009 USDA. Soil and Water Research Laboratory/Blackland Research Center, Texas, USA

Olivera F, Valenzuela M, Srinivasan R, Choi J, Cho H, Koka S, Agrawal A (2006) ArcGIS-SWAT: a geodata model and GIS interface for SWAT. J Am Water Resour Assoc 42:295–309

Palazón L, Navas A (2011) Application and validation of SWAT model to an alpine catchment in the Central Spanish Pyrenees. In: Kiniry D, Smith C, Srinivasan R (eds) 2011 International SWAT Conference—Conference Proceedings. Toledo, USA, pp 162-172

Palazón L, Navas A (2013) Sediment production of an alpine catchment with SWAT. Z Geomorphol 57:69–85

Rahman K, Maringanti C, Beniston M, Widmer F, Abbaspour K, Lehman A (2013) Streamflow modeling in a highly managed mountainous glacier watershed using SWAT: the Upper Rhone River watershed case in Switzerland. Water Resour Manag 27:323–339

Rijckborst H (1967) Hydrology of the Upper Garonne basin (Valle de Arán, Spain). Leidse Geol Meded 40:1–74

Rostamian R, Jaleh A, Afyuni M, Mousavi SF, Heidarpour M, Jalalian A, Abbaspour KC (2008) Application of a SWAT model for estimating runoff and sediment in two mountainous basins in central Iran. Hydrol Sci J 53:977–988

Stratton BT, Sridhar V, Gribb MM, McNamara JP, Narasimhan B (2009) Modeling the spatially varying water balance processes in a semi-arid mountainous watershed of Idaho. J Am Water Resour Assoc 45: 1390–1408

SWAT (2011) Soil and Water Assessment Tool: SWAT model software. US Department of Agriculture-Agricultural Research Service, Grassland, Soil & Water Research Laboratory, Temple, Texas, USA, Available at: http://swatmodel.tamu.edu/software/swat-model/

Valero-Garcés BL, Navas A, Machín J, Walling D (1999) Sediment sources and siltation in mountain reservoirs: a case study from the Central Spanish Pyrenees. Geomorphology 28:23–41

Vicente-Serrano SM, Beguería S, López-Moreno JI, García-Vera MA, Stepanek P (2009) A complete daily rainfall database for north-east Spain: reconstruction, quality control and homogeneity. Int J Climatol 30:1146–1163

Verdú JM, Batalla RJ, Martínez-Casasnovas JA (2006a) Estudio hidrológico de la cuenca del río Isábena (Cuenca del Ebro) I: Variabilidad de la precipitación. Ing Agua 13:321–330

Verdú JM, Batalla RJ, Martínez-Casasnovas JA (2006b) Estudio hidrológico de la cuenca del río Isábena (Cuenca del Ebro) II: Respuesta hidrológica. Ing Agua 13:331–344

Williams JR (1995) Chapter 25: The EPIC model. In: Singh VP (ed) Computer models of watershed hydrology. Water Resources Publications, Highland Ranch, Colorado, USA, pp 909–1000

Yu M, Chen X, Li L, Bao A, de la Paix MJ (2011) Streamflow simulation by SWAT using different precipitation sources in large arid basins with scarce raingauges. Water Resour Manag 25:2669–2681

Zhang X, Srinivasan R, Debele B, Hao F (2008) Runoff simulation of the headwaters of the Yellow River using the SWAT model with three snowmelt algorithms. J Am Water Resour Assoc 44:48–61

Tables:

Table 1.- Spatial input data used for the Barasona catchment in SWAT.

Spatial input	Source	Resolution	Database input	Observations/editions
DEM	National Geographic Institute (IGN 2011)	25 m		5 slope categories: 0-20 %, 20-40 %, 40-60 %, 60-75 % and >75 %
Land cover map	European Project Corine Land Cover map (CLC2000)	100 m resampled to 25 m	SWAT2009 crop table	Edited to introduce the spatial extend of the badlands
Soil map	Digital Soil Map of Aragón (Soil Map of Aragón, 1:500,000, Machín J, unpublished 2000)	25 m	User soil database within SWAT2009	Edited to introduce the spatial extend of the bare rock and badlands

Table 2.- Hydrological context of the study years (2003-2006) within the 30 years record of the available rainfall and gauge stations.

		30 years	2003-2006	2003	2004	2005	2006
Graus gage	Streamflow (m^3s^{-1})	17.4 ±11.2	18.1	26.7	16.1	11.3	18.4
	Runoff (hm^3)	550 ±138	572	842	509	357	581
	Return period (year)			21.8	1.8	1.1	2.8
Capella gage	Streamflow (m^3s^{-1})	4.4±4.4	3.6	6.2	3.6	1.3	3.3
	Runoff (hm^3)	138±66	113	196	114	40	103

	Return period (year)			5.3	1.7	1	1.5
Rainfall (mm)	Mediano	771	673	922	528	587	655
	Eriste	1087	967	1278	715	887	988
	Sesue	1047	986	1311	810	857	965
	Serraduy	720*	686	909	629	513	693

*continuous daily data for the 1987-2006 period

Table 3.- Range, default and final calibrated values of selected SWAT model parameters

	Parameter	SWAT range	Default Value	Fitted value
Snow	Snow fall temperature, SFTMP (°C)	-5 to 5	1	1.5
	Snowmelt temperature, SMTMP (°C)	-5 to 5	0.5	4.3
	Maximum melt rate of snow during a year, SMFMX (mm $°C^{-1}$ day^{-1})	0 - 10	4.5	1.5
	Minimum melt rate of snow during a year, SMFMN (mm $°C^{-1}$ day^{-1})	0 - 10	4.5	0.1
	Snow pack temperature lag factor (TIMP)	0 - 1	1	0.1
	Minimum snow water content at 100% snow cover, SNOCOVMX (mm)	0 - 500	1	200
	Snow water equivalent at 50% snow cover, SNO50COV	0 – 1	0.5	0.1
Groundwater	Initial depth of water in the shallow aquifer, SHALLST (mm H_2O)	100-50000	0.5	100
	Initial depth of water in the deep aquifer, DEEPST (mm H_2O)	1000-50000	1000	1000
	Groundwater delay, GW_DELAY (days)	0-500	31	31
	Baseflow alpha factor, ALPHA_BF (days)	0-1	0.048	0.02
	Threshold depth of water in the shallow aquifer required for return flow to occur, GWQMN (mm H_2O)	0-5000	0	300

	Groundwater "revap" coefficient, GW_REVAP	0.02-0.2	0.02	0.02
	Threshold depth of water in the shallow aquifer for "revap" to occur, REVAPMN (mm H_2O)	0-500	1	0
Channel	Manning's "n" roughness value for the main channel, CH_N2	-0.01 to 0.3	0.014	0.08
	Manning's "n" roughness value for the tributary channel, CH_N1	0.01 to 30	0.014	0.03
Sediment transportation	Linear parameter for calculating the maximum amount of sediment that can be re-entrained during channel sediment routing, SPCON	0.0001 - 0.01	0.0001	0.001

Table 4.- Observed and simulated streamflow at Graus and Capella gauge stations and simulated average annual precipitation, surface runoff and water yield for the Barasona catchment (max: maximum; min: minimum; sd: standard deviation).

		mean	max	min	sd	2003	2004	2005	2006
Graus	Observed	18.1	47.2	4.8	10.9	26.7	16.1	11.3	18.4
	Simulated	18.0	42.0	1.9	9.6	25.6	17.0	12.6	17.2
Capella	Observed	3.6	16.6	0.6	3.4	6.2	3.6	1.3	3.3
	Simulated	4.5	13.9	0.5	3.0	6.4	4.7	2.6	4.5
Barasona (mm)	Precipitation	1039	1383	871	239	1383	882	871	1021
	Surface runoff	115	172	85	40	172	86	85	118
	Water yield	541	769	350	165	769	527	350	516

Max maximum, Min minimum, SD standard deviation

Table 5.- Simulated sediment yield (SY) and specific sediment yield (SSY) for the Barasona catchment in the study years and contributions from the Ésera and Isábena rivers.

year	SY	SSY	Ésera contribution		Isábena contribution	
	t $year^{-1}$	t ha^{-1} $year^{-1}$	t ha^{-1} $year^{-1}$	(SY %)	t ha^{-1} $year^{-1}$	(SY %)
2003	1 135 000	8.25	9.05	65	10.03	35
2004	547 000	3.98	4.40	67	4.45	33
2005	378 000	2.74	3.32	71	2.78	29
2006	515 000	3.74	4.22	68	4.04	32

Table 6.- Specific Sediment Yield (SSY: t ha^{-1} $year^{-1}$) by Pyrenean Structural Units.

	2003	2004	2005	2006
Axial Pyrenees	23.3	3.8	4.0	6.7
Internal Ranges	32.2	13.3	12.5	11.7
Internal Depressions	462.1	181.9	139.5	147.1
Intermediate Depression	38.4	20.1	15.6	23.8
External Ranges	8.4	9.2	5.3	9.5

Table 7.- Average monthly simulated suspended sediment concentration (SSC) of the main rivers at the limit of the Pyrenean Structural Units for the study period (2003-2006).

	Ésera River					Isábena River				
	period	2003	2004	2005	2006	period	2003	2004	2005	2006
	$g\ l^{-1}$					$g\ l^{-1}$				
Axial Pyrenees	0.090	0.153	0.116	0.044	0.048	0.032	0.029	0.023	0.027	0.022
Internal Ranges	0.213	0.211	0.224	0.184	0.191	0.109	0.107	0.101	0.105	0.102
Internal Depressions	0.484	0.472	0.462	0.403	0.403	0.819	0.797	0.783	0.586	0.575
Intermediate Depression	0.528	0.522	0.521	0.432	0.478	0.647	0.629	0.636	0.480	0.498
Barasona reservoir main inflow	0.509	0.683	0.506	0.397	0.449					

Table 8.- Statistics for the SSY of the subcatchments ($t\ ha^{-1}\ year^{-1}$) within each Pyrenean Structural Units (m: mean; mn: median; sd: standard deviation).

	2003-2006			2003			2004			2005			2006		
	Mean	Median	SD	Mean	Median	SD	Mean	Median	SD	Mean	Median	SD	Mean	Median	SD
Axial Pyrenees	0.6	0.3	0.8	1.5	1.6	1.5	0.2	0.1	0.2	0.2	0.1	0.2	0.4	0.4	0.4
Internal Ranges	2.2	0.8	2.8	4.0	2.0	4.4	1.7	0.7	2.1	1.6	0.7	2.0	1.5	0.7	1.7
Internal Depressions	29.1	21.2	32.7	57.8	53.7	52.0	22.7	22.6	18.3	17.4	17.4	14.5	18.4	17.9	15.0
Intermediate Depression	1.5	1.4	1.2	2.4	2.3	1.6	1.3	0.9	1.1	1.0	0.9	0.7	1.5	1.6	1.0
External Ranges	0.9	0.9	0.5	0.9	1.0	0.5	1.0	1.1	0.4	0.6	0.7	0.3	1.1	1.2	0.5

SD standard deviation

Fig. 1 Location in the Ebro Basin, Spain, and maps of the characteristics (position of dams, Jueu karst system, and climate stations), soils, and digital elevation model (DEM) of the Barasona catchment

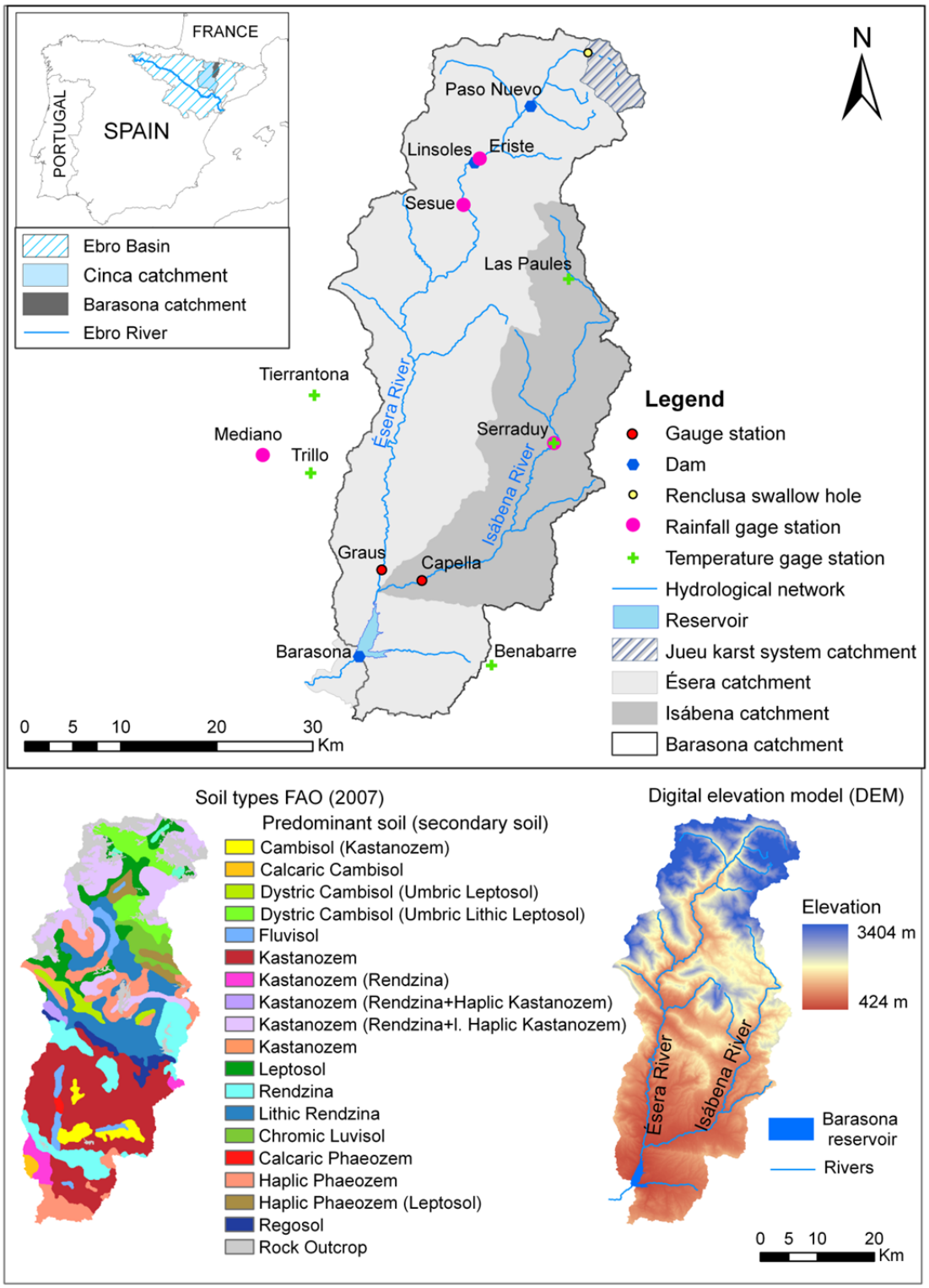

Fig. 2 Lithological distribution and characteristics of the Pyrenean structural units in the Barasona catchment. Map shows slope ranges, competent or non-competent lithologies, and agricultural and non-agricultural field distributions

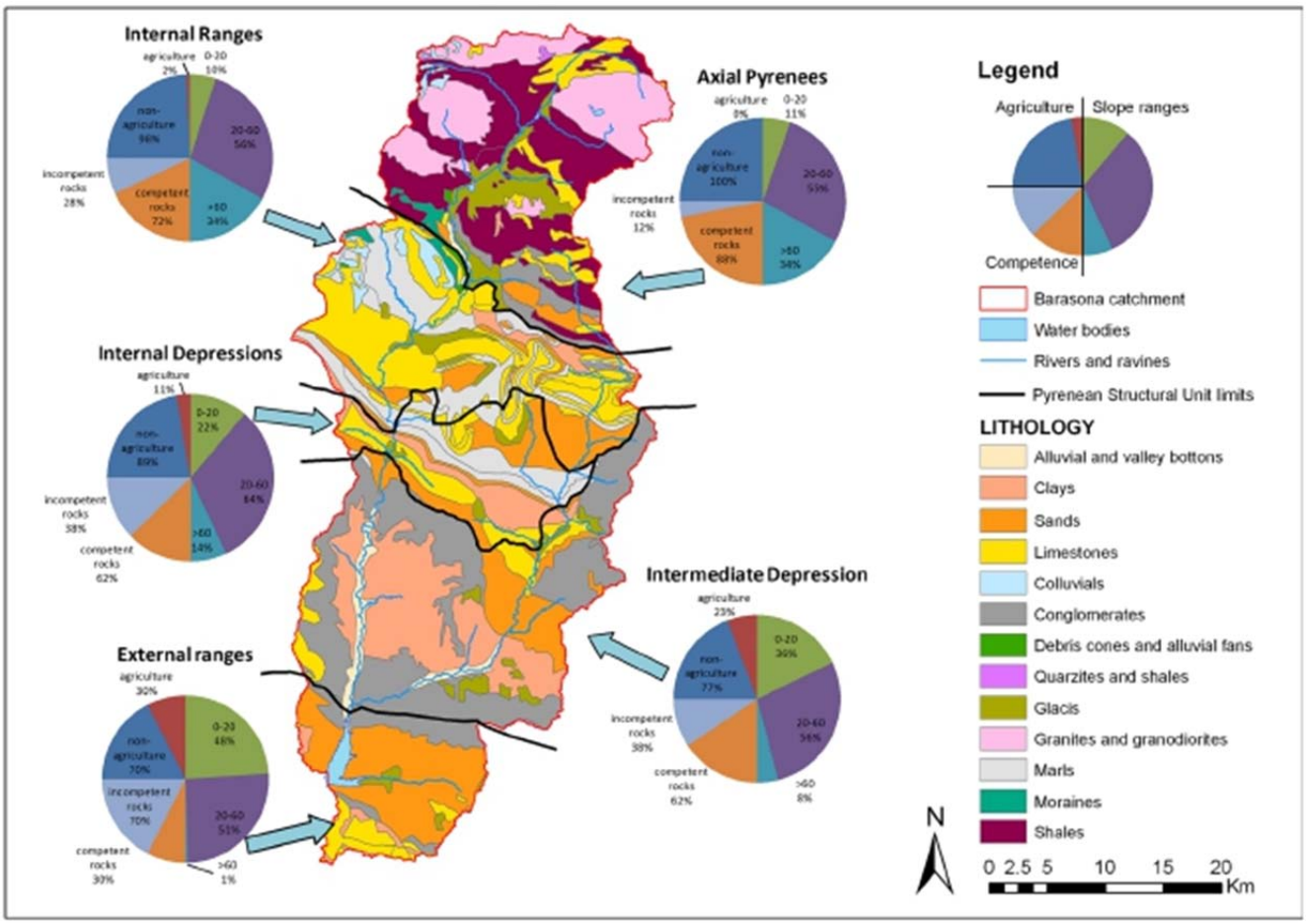

Fig. 3 Observed and simulated monthly hydrographs and simulated sediment yield for the Graus and Capella river gauging stations

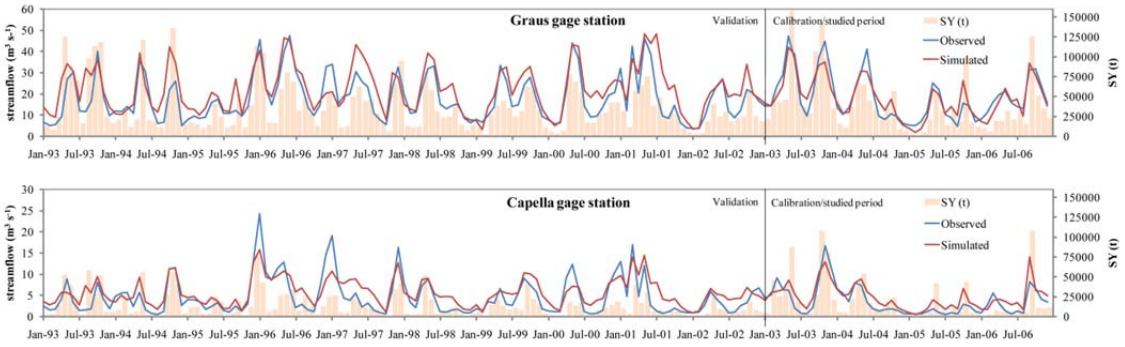

Fig. 4 Spatial and temporal variability of specific sediment yield (SSY) for the subcatchments of the Barasona catchment for the study years (2003–2006)